J Fluoresc (2015) 25:1763–1773
DOI 10.1007/s10895-015-1664-4

ORIGINAL ARTICLE

A New Isoindoline Based Schiff Base Derivative as Cu(II) Chemosensor: Synthesis, Photophysical, DNA Binding and Molecular Docking Studies

Pattan Sirajuddin Nayab [1] · Madhusudana Pulaganti [2] · Suresh Kumar Chitta [2] · Rahisuddin [1]

Received: 5 June 2015 / Accepted: 14 September 2015 / Published online: 26 September 2015

Abstract A new chemo sensor 2-(4-methylbenzylideneamino)-isoindoline-1,3-dione (PDB) was synthesized and characterized by UV–Vis., IR, ^{1}H NMR, ^{13}C NMR spectral and elemental analysis. Its photophysical properties in organic solvents with different polarity were studied. The sensitivity of the PDB in different pH solutions was investigated and the results indicated that PDB would be able to act as an efficient "off–on–off" switch for pH. This chemosensor displayed high selectivity towards Cu^{2+} in the presence of metal ions Ba^{2+}, Cd^{2+}, Co^{2+}, Hg^{2+}, Ni^{2+}, Pb^{2+}, K^{+} and Zn^{2+} in DMF/H_2O solution. Furthermore DNA binding and molecular docking studies were also carried out to investigate the biological potential of the test compound. The interaction of compound (PDB) with Ct-DNA was examined by absorption, CD spectroscopy, cyclic voltammetry and viscosity measurements. In silico studies revealed that the test compound (PDB) showed good affinity towards the target receptor d $(CGCGAATTCGCG)_2$ with the binding energy of −7.70 kcal/mol.

Keywords Phthalimide · pH sensor · Cu(II) sensor · Molecular modeling · Ct-DNA binding studies

Electronic supplementary material The online version of this article (doi:10.1007/s10895-015-1664-4) contains supplementary material, which is available to authorized users.

✉ Rahisuddin
rahisuddin@jmi.ac.in

[1] Department of Chemistry, Jamia Millia Islamia, New Delhi 110 025, India

[2] Department of Biochemistry, Sri Krishnadevraya University, Ananthapuram 515 003, India

Introduction

Over the past years, design and development of molecular sensors for the detection of anions and cations has been the subject of great interest in research due to their high sensitivity and rapid response. Copper is an essential biometal considered as the third most abundant trace element in the human body after iron and zinc, plays a vital role in a variety of physiological processes including oxygen transportation, hormone maturation, signal transduction [1]. Though copper is a significant component due to its established role in biological systems, accumulation of high doses of copper is extremely toxic [2]. Therefore, there is a considerable need for the development of novel methods to recognize the copper ions in biological and chemical systems. A variety of techniques has been reported to detect Cu^{2+} ions such as atomic absorption spectrometry (AAS), inductively coupled plasma-atomic emission spectrometry (ICP-AES) and inductively coupled plasma-mass spectrometry (ICP-MS) [3–5]. However enormous cost of infrastructure maintenance and operative expenditure related to these techniques has stimulated the search for new methods. In recent years, photo physical methods for the detection of metal ions have attracted tremendous attention because of their highly sensitivity, specificity, simplicity and low-cost instrumentation [6, 7]. Literature is enriched with a number of mechanisms for sensing signaling processes such as intra-molecular charge transfer, photo-induced electron transfer (PET), excimer/exciplex formation, ground-state charge transfer and excited-state proton transfer [8].

Schiff bases containing nitrogen and other donor atoms have been extensively studied in coordination chemistry. Schiff bases also gained significant interest in medicinal chemistry because they have potential antibacterial [9], antifungal [10], and antiviral applications [11]. A great number of

Schiff bases have been demonstrated as molecular sensors for the recognition of metal ions due to their ability to completely bind metal ions and to stabilize them in various oxidation states. Recently, copper selective fluorescent probe has been reported by Kumar et al. [12]. Shellaiah and co-workers reported an anthracene-based Schiff base fluorescent turn-on sensor for copper [13]. Since Cu^{2+} is a paramagnetic nature, it quenches fluorescence emission of nearly all fluorophores through electron or energy transfer mechanism [14].

Phthalimides are an important class of heterocyclic compounds has received special attention of chemists in organic, medicinal, analytical and coordination chemistry. Phthalimide and their derivatives possess a wide range of biological activities including antimicrobial [15], antitumour [16] and DNA cleaving activities [17]. Several phthalimide containing compounds have also been described as molecular sensors for the recognition of cations and anions [18]. This may be attributed to their photostability, high fluorescence yields, strong absorption and emission in the UV–vis. region. Recently, 4-benzoylamido-N-methylphthalimide and urea activated phthalimide chemosensor has been designed and developed for selective detection of fluoride ions (Fig. 1) [19, 20]. Based on the above considerations, in this article we report a novel chemosensor sensitive to solvent polarity, pH and selective to Cu^{2+} ions. To the best of our information, there has been no report on the development of chemosensor for monitoring Cu^{2+} ions based on phthalimide derivatives conjugated to the Schiff base moiety.

Various analytical methods have been employed for the detection of DNA-drug interactions ranging from fluorescence spectroscopy [21], UV-visible spectroscopy [22], nuclear magnetic resonance [23], electrochemistry [24], circular dichroism [25] and hydrodynamic measurements [26]. The efficiency of anticancer drugs may be attributed to their DNA-interacting capabilities. Therefore, investigating the interactions of small molecules with DNA has been paid more attention in the cancer chemotherapy. Molecular docking study occupied a unique position in modern drug designing, as it provides detailed information about drug-receptor interactions to predict the binding orientation of drug candidates to their target proteins [27]. To provide an insight into biological efficacy of newly synthesized molecule, it was also subjected to DNA binding and docking studies against dodecamer $d(CGCGAATTCGCG)_2$.

Herein, we describe the synthesis and spectroscopic properties of phthalimide derivative containing Schiff base moiety for detection of Cu^{2+} ions. In the present study, cyclic voltammetry, viscosity measurements, UV–visible and CD spectroscopic techniques are used to determine binding modes, hydrodynamic and conformational changes of PDB-DNA complexes in ethanol solution.

Experimental Section

Materials and Methods

All reagents were used as purchased from Sigma-Aldrich. The solvents were of spectroscopy grade and used without further treatment. The reaction was monitored by thin layer chromatography using UV cabinet for visualization. Yield percent was of purified product and was not optimized. Melting point was recorded using an electro-thermal melting point apparatus and were uncorrected. Electronic spectra were obtained on a Perkin Elmer Lamda 40 UV-Visible spectrophotometer. IR spectra were recorded in the range of 4000–400 cm^{-1} on a Perkin Elmer Spectrum RXI IR Instrument as KBr discs. ^1H NMR spectra were recorded on Bruker DPX-300 NMR spectrometer operating at 300 MHz using DMSO-d_6 as solvent. Fluorescence spectra were achieved with Jobin-Yvon Fluorolog 3–22 spectrofluorometer using 450 W xenon lamp and R928P PMT as the excitation source and detector, respectively. CD spectra were obtained on a Chirascan CD spectropolarimeter. Cyclic voltammetry measurements were made on a DY2312 potentiostat.

Synthesis

Preparation of 2-(4-methylbenzylideneamino) -isoindoline-1,3-dione (PDB)

N-aminophthalimide (0.324 g, 2 mmol) was suspended in boiling glacial acetic acid (20 mL), followed by the addition of solution of *p*-dimethylamino benzaldehyde (0.30 g, 2 mmol) in ethanol (15 mL). The reaction mixture was stirred with heating for 6 h. After cooling the solution, the resulting brown precipitate was filtered, washed with cold ethanol. Finally the compound dried in a vacuum desiccator over fused calcium chloride. Brown solid; Yield 64 %; mp: 242 °C; UV λ_{max} (nm): 340, 235; IR $_{max}$ (cm^{-1}): 2948, 2831 (C-H), 1773, 1704 (C=O), 1544 (C=N), 724 (Ar-H); ^1H NMR (300 MHz, DMSO-d_6) δ in ppm: 8.843 (s, 1H, N=CH), 8.031–8.133 (m, 2H, Ar-H), 7.833–7.863 (d, 2H, J=9.0 Hz, Ar-H), 7.658–7.687 (d, 2H, J=8.7 Hz, Ar-H), 6.773–6.802 (d, 2H, J=8.7 Hz, Ar-H), 3.012 (s, 6H, N-CH_3); ^{13}C NMR (100 MHz, $CDCl_3$) δ in ppm: 166.52,154.34, 149.61, 134.23, 131.95, 130.27, 125.16, 123.42, 110.98, 40.02; Anal. Calcd. for $C_{17}H_{15}N_3O_2$ (293.12): C, 69.61; H, 5.15; N, 14.33. Found: C, 69.65; H, 5.13; N, 14.29.

DNA Binding Studies

Absorbance Measurements

The absorption spectral titrations were performed in Tris–HCl/NaCl buffer (0.01 M, pH 7.2) by varying the concentrations of the DNA while fixing the sample concentration at 4.2×10^{-5} M. The absorption spectra were measured at

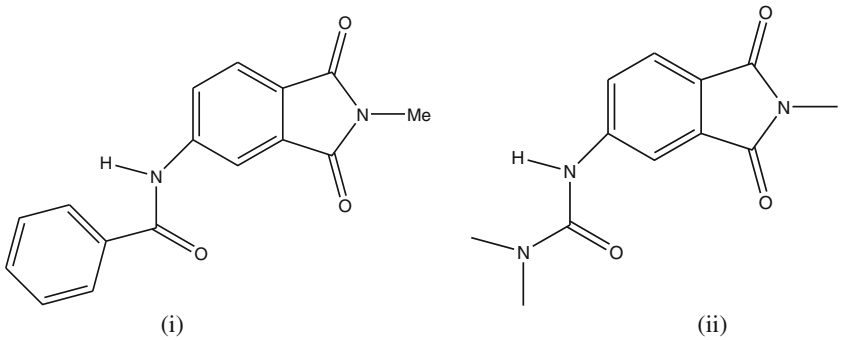

Fig. 1 Structure of (i) 4-benzoylamido-N-methylphthalimide (ii) urea activated phthalimide

298 K over a wavelength range of 190–400 nm. The concentration of Ct-DNA in the stock solution was determined by UV absorbance at 260 nm by taking the molar extinction coefficient value ε_{260}=6600 L mol^{-1} cm^{-1}. The absorbance of Ct-DNA in buffer at 260 and 280 nm gave a ratio of 1.9:1 indicating that DNA was free from protein. The solutions were allowed to equilibrate for 10 min before the absorption spectra were recorded. Equal amount of DNA was added to both the reference and the test solutions to eliminate the absorbance of nucleic acid itself at the measured wavelength.

Circular Dichroism Spectra Studies

Circular dichroic experiments were carried out using a rectangular quartz cell of 1 cm path length at 20±0.5 °C. The CD spectra of Ct-DNA (25 mM) in the absence and presence of the test compound (25 mM) were determined at room temperature in 5 mM Tris–HCl/ 50 mM NaCl buffer (pH 7.2) Each CD spectrum was obtained by averaging three successive scans and all observed CD profiles were corrected for the buffer signal.

Viscosity Measurements

The viscosity of Ct-DNA in the absence and presence of the target compound in the 5 mM Tris–HCl/ 50 mM NaCl buffer solution (pH=7.2) was measured using Ostwald capillary viscometer maintained at 25±0.1 °C. Hydrodynamic measurements were performed by maintaining the DNA concentration (4×10^{-5} M) as constant while varying the concentration of the compound within the range of 0.4–1.6×10^{-5} M. The data were reported as $(\eta/\eta^o)^{1/3}$ versus the molar ratios, where η^o and η are the specific viscosities of Ct-DNA alone and the PDB−Ct-DNA complex. Viscosity values were determined from the observed flow time of DNA-containing solutions (t) and corrected for buffer solution (t_0), $\eta=(t-t_0)/t_0$.

Electrochemical Studies

Electrochemical studies were performed in a single compartment cell with a three-electrode configuration, glassy carbon working electrode, platinum wire auxiliary electrode and saturated calomel as a reference electrode. The glassy carbon electrode was polished with alumina powder and the solution was deoxygenated with nitrogen gas for 20 min prior to each experiment. Cyclic voltammetry for compound (PDB) was carried out in the absence and presence of DNA in Tris-buffer (pH 7.5) and NaCl (20 mM) as supporting electrolyte. All the experiments were carried out at a scan rate 50 mVs^{-1} in the potential range +1.0 to −1.0 V at room temperature.

Molecular Docking Studies

Docking studies of PDB were carried out on the dodecamer d(CGCGAATTCGCG)$_2$ (PDB ID: 1BNA), to determine the biological efficiency of this compound. The ligand was sketched in ChemDraw Ultra 8.0 assigned with proper 2D orientation (ChemOffice package) and was converted to energy minimized 3D structures for in silico protein–ligand docking using "AutoDock Tools" [28]. The Protein Data Bank retrieved crystal structure of the synthetic DNA dodecamer d(CGCGAATTCGCG)$_2$ (PDB ID: 1BNA) [29]. The docking parameters including free binding energy, electrostatic energy, intermolecular energy and torsional free energy were calculated.

Results and Discussion

Chemistry

We report here an efficient method for the synthesis of novel phthalimide derivative (PDB) was given in Scheme 1. The electronic spectra of the synthesized compound were recorded in the range 200–600 nm in EtOH solvent. In particular, the bands appeared in the UV–Vis. spectrum of PDB at 300–400 nm can be attributed to the excitation of electrons of azomethine C=N group [30]. In this study, the peak observed at 240 nm is attributed to the π-π* transition of the phenyl rings and

Scheme 1 Synthetic procedure of 2-(4-methylbenzylideneamino)-isoindoline-1,3-dione (PDB)

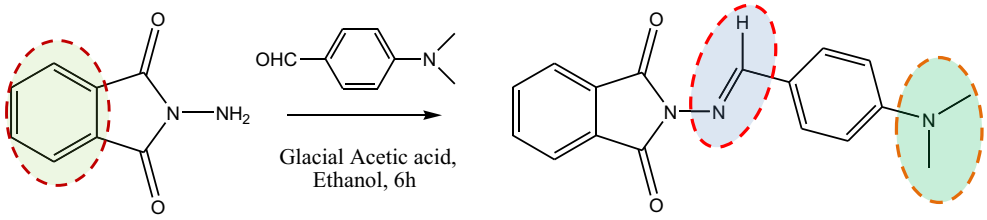

352 nm peak is assigned to the π-π* transition of azomethine (CH=N) group.

The FT-IR spectra of the title compound were recorded in the 4000–400 cm^{-1} region. The IR spectrum of the synthesized compound exhibited characteristic signal at 1544 cm^{-1}, which is assigned to the azomethine group corroborated well with the proposed structure. The bands observed at 1704–1773 cm^{-1}, can be attributed to C=O stretching vibrations (See supporting information, Fig. S1).

The ^{1}H NMR spectra were recorded in DMSO-d_6 solvent and representative spectra is given in Fig. 2. ^{1}H NMR spectrum of compound (PDB) showed two doublet peaks at 7.68 and 6.80 correspond to aromatic protons. The phthalimide ring protons exhibit multiplets in 8.13–7.83 ppm range. While a sharp signal appears at 3.01 ppm corresponds to CH_3 proton. The signal due to azomethine group observed as singlet at 8.84 ppm indicates the formation of Schiff base compound. Furthermore, the appearance of a signal at 149 ppm in the ^{13}C NMR spectrum of PDB confirms the formation of proposed Schiff base framework. The aromatic signals for PDB were observed in 110–134 ppm range. Moreover, the signal due to CH_3 was obtained at 40 ppm.

The Influence of Solvents on UV–vis. and Fluorescence Spectra

The photophysical sensitivity of PDB towards various solvents of different polarity was studied in order to find out its spectral properties in organic solvents. The absorbance and fluorescence spectra of PDB in different solvents were shown in Fig. 3 and its photophysical characteristics were presented in Table 1. It can be clearly seen from Fig. 3 that upon increasing the polarity of the solvent there was a red-shift in absorbance and fluorescence maxima of compound PDB. For example, the maximum absorption in acetone and dimethyl formamide was located at 356 nm whereas the maximum absorption in diethyl ether and cyclohexane has a blue shift in a range of 8 nm respectively. In addition, it exhibited strong fluorescence in nonpolar solvents such as cyclohexane and diethyl ether while in polar solvents, the fluorescence intensity of compound (PDB) was considerably diminished. The observed bathochromic shift in polar solvents, indicating that the singlet excited state is more polar than the ground state.

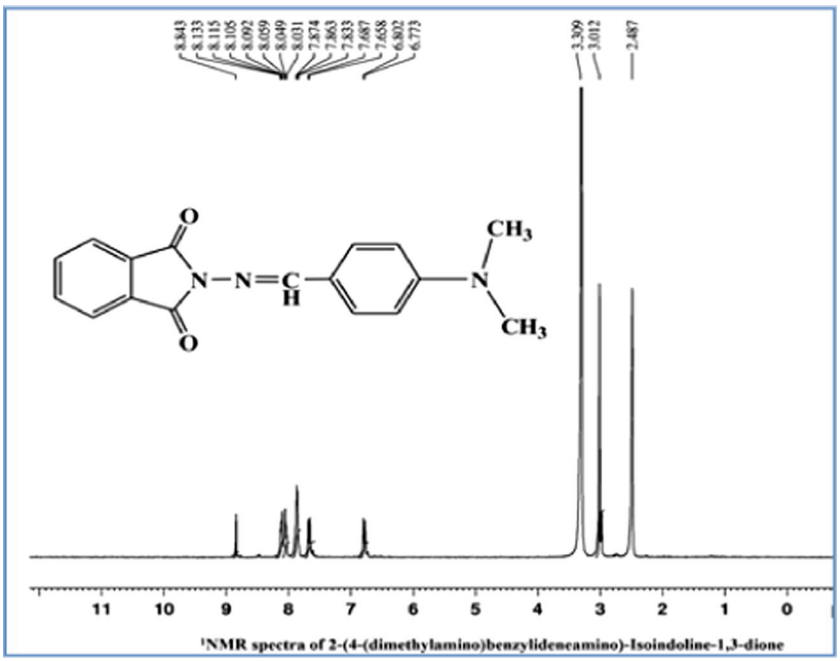

Fig. 2 ^{1}H NMR spectra of 2-(4-(dimethylamino)benzylideneamino)-Isoindoline-1,3-dione (PDB)

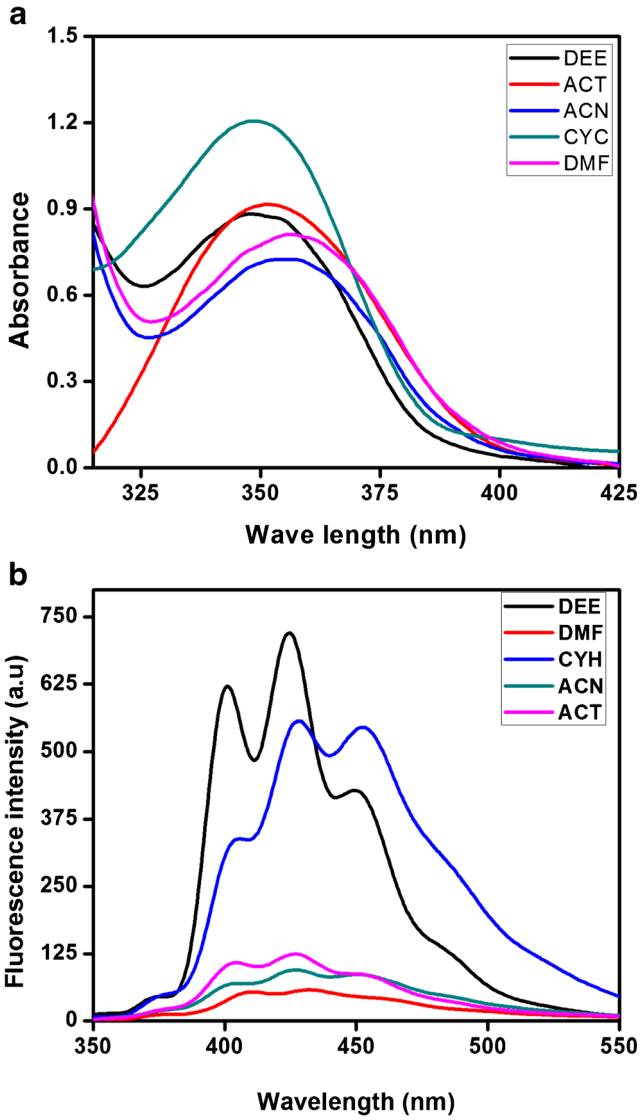

Fig. 3 **a** Absorbance spectra of the PDB. **b** Fluorescence emission spectra of PDB in different solvents

Since the dipole moment of the molecule is increased upon excitation, the excited molecule is better stabilized in polar solvent, due to large dipole–dipole interactions and intermolecular hydrogen bonds between PDB and solvent molecules [31].

Table 1 Photophysical characteristics of compound PDB in different solvents

Solvent	λ_{abs} (nm)	Absorbance	λ_{flo} [a] (nm)	Intensity
DEE	347.5	0.883	424	778.7
CYH	348.5	1.207	427	582.7
ACT	351.5	0.916	425	130.7
ACN	356.5	0.726	427.5	101.3
DMF	356	0.812	431	61.89

[a] Fluorescence maxima at λ_{ex}=340 nm

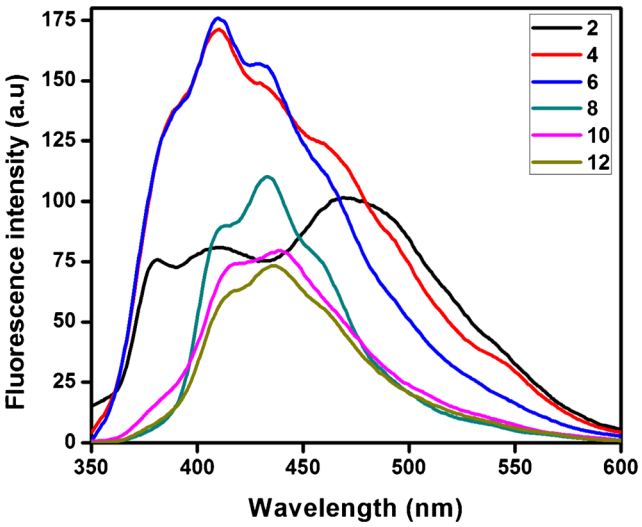

Fig. 4 Fluorescence spectra of the compound PDB in different pH

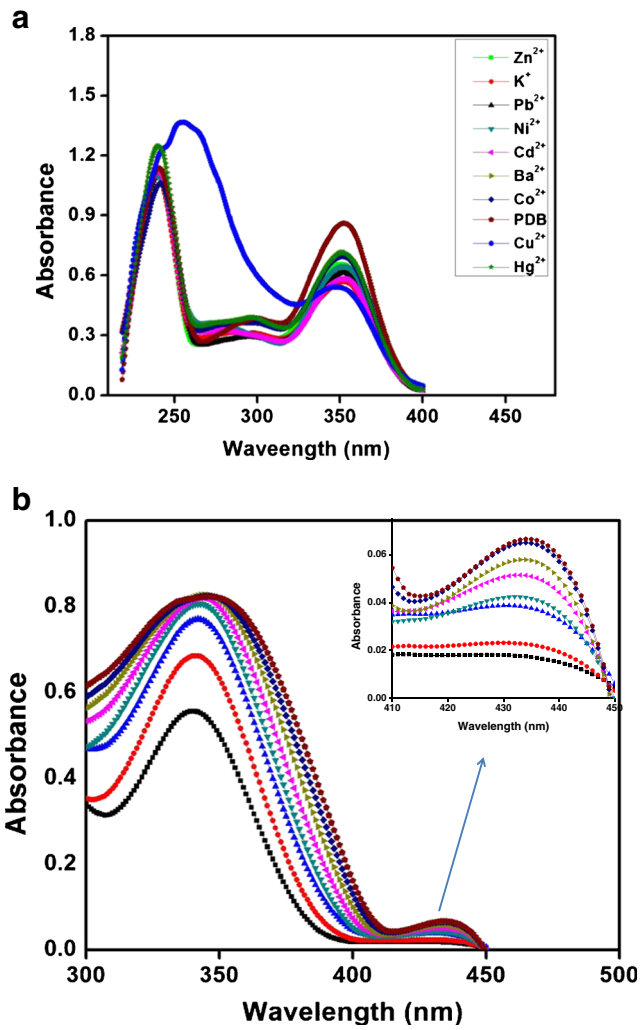

Fig. 5 **a** The absorption spectrum of PDB and in the presence of different metal ions (5 eq) in DMF/ H_2O (1:1, *v/v*); **b** The absorption spectrum of PDB in ethanol solution at different $[Cu^{2+}]$=(1, 2.5, 5, 6.5, 7.5, 8.5, 9 and 10 eq.); [PDB]=1.2×10^{-5} M

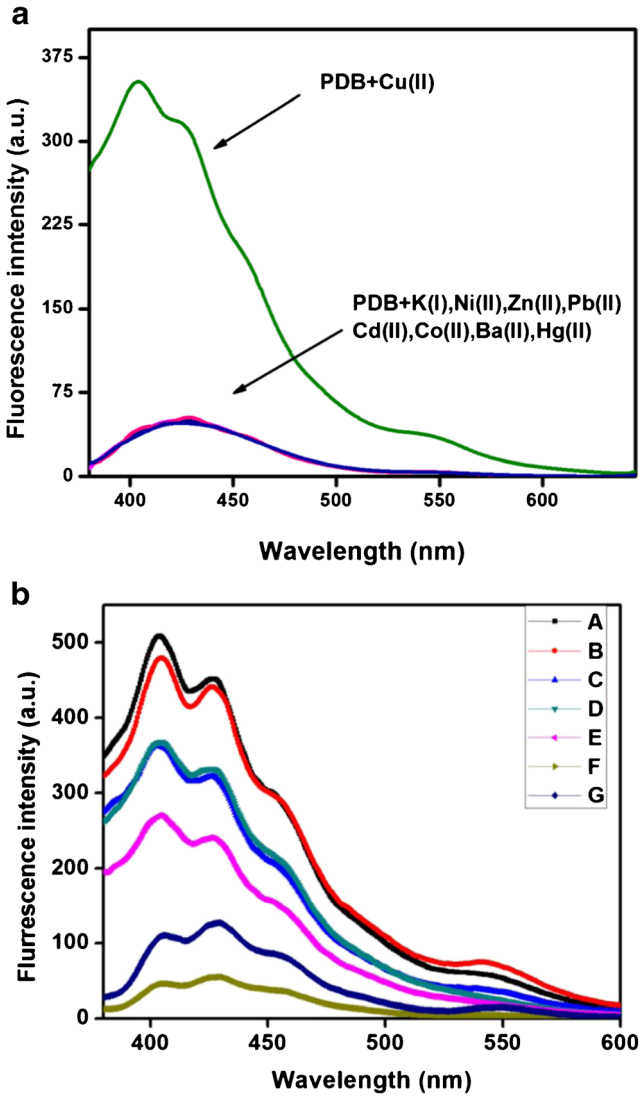

Fig. 6 **a** The fluorescence spectrum of PDB and in the presence of different metal ions (5 eq) DMF/ H_2O (1:1, *v/v*). **b** The fluorescence spectrum of PDB in ethanol solution at different [Cu^{2+}] (1, 2.5, 5, 6.5, 7.5, 8.5 and 10 eq); [PDB]=1.2×10^{-5} M

The Effect of pH on the Fluorescence Spectra

The effect of pH on its fluorescence spectra was studied in a range from 2 to 12. As can be seen from the Fig. 4, the fluorescence emission of the probe in acidic medium is low. Upon increasing the pH of the medium from 2 to 6, the emission became blue shifted with greater intensity enhancement. While in 6 to 8 pH range, the enhanced fluorescence intensity was gradually decreased. However, further increasing from 8 to 12 the fluorescence intensity of PDB decreased significantly. The changes in the fluorescence intensity as a function of pH for compound PDB was probably due to the protonation of imine (C=N) nitrogen that would affect the ICT interaction, subsequently the emission would be quenched in the acidic medium. The quenching of the luminescence of the test compound could be also attributed to the damage of C=N bond of Schiff base in low or high pH value [32]. The fluorescence intensity of PDB displayed steady signals in the pH range from 4 to 8. Therefore, the experiments followed have been carried out in nearly neutral solution of pH 6.8.

Selectivity and Sensitivity of PDB to Metal Ions

Absorbance Spectroscopic Studies

The absorbance sensitivity of PDB towards metal ions such as Ba^{2+}, Cd^{2+}, Co^{2+}, Hg^{2+}, Cu^{2+}, Ni^{2+}, Pb^{2+}, K^{+} and Zn^{2+} was primarily investigated. The absorbance spectrum of PDB displayed two characteristic peaks at 240 and 352 nm in DMF/ H_2O solution. As can be seen in Fig. 5, upon addition of 5 equivalents of metal ions Ba^{2+}, Cd^{2+}, Co^{2+}, Hg^{2+}, Cu^{2+},

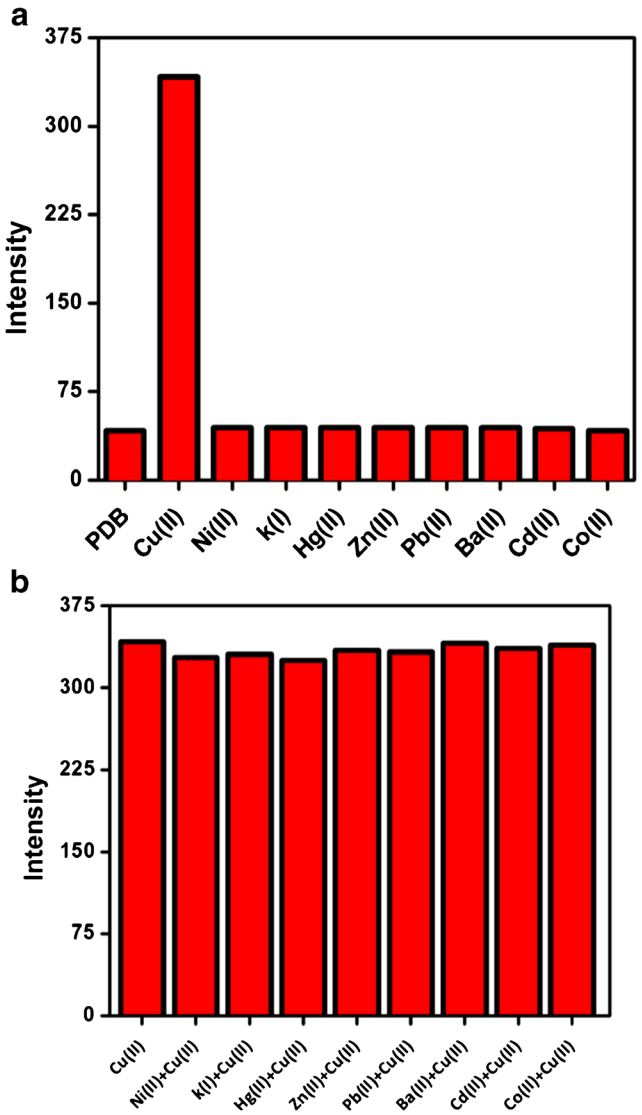

Fig. 7 **a** Histogram representing emission intensity at 410 nm of PDB upon addition of various metal ions (5 eq). **b** Intensity changes in the presence of the competing metal ions

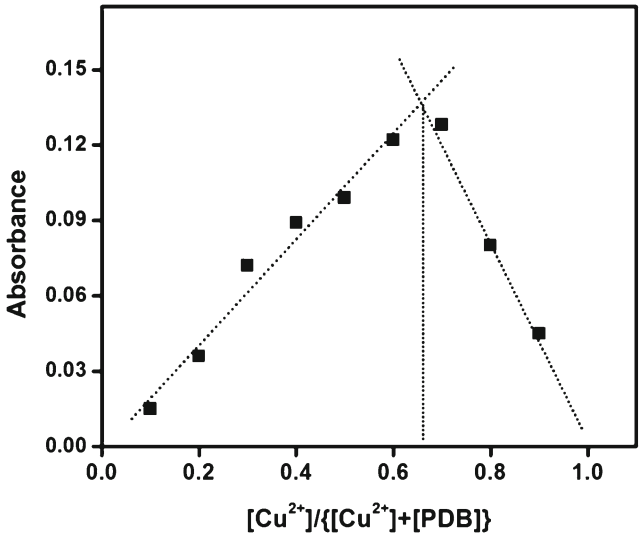

Fig. 8 Job's plot for Cu^{2+}-PDB system $[Cu^{2+}]+[PDB]=1.0\times10^{-5}$ mol L^{-1}

Ni^{2+}, Pb^{2+}, K^{+} and Zn^{2+} to the solution containing 1 equivalent of PDB, a slight decrease in band intensity with no marginal shift in peak positions was observed. However upon the addition of Cu^{2+} with the same concentration, a marginal bathochromic shift of the band at 240 with a slight decrease in band intensity in the absorption band at 352 was observed. Furthermore, with the progressive addition of various concentrations of Cu^{2+} ions to ethanol solution of PDB with a fixed concentration, the absorbance of PDB at 340 nm was gradually increased with a concomitant new peak centered at 430 nm The enhanced absorption appeared around 340 nm is due to binding of phthalimide derivative on Cu metal ion. Moreover, a new absorption band at 430 nm emerged gradually along with the addition of increased amounts of copper (II) ions (inset of Fig. 5b). According to the above data, we can conclude that among the various tested metal ions, copper exhibits considerably stronger complexation with the probe.

Fluorescence Spectroscopic Studies

The sensitivity of PDB towards Cu^{2+} over other transition metals was further investigated by means of flouremetric titrations. The fluorescence spectrum of PDB displayed characteristic peak at 410 nm. As can be seen in the Fig. 6a, no Significant spectral changes were observed in the presence of Ba^{2+}, Cd^{2+}, Co^{2+}, Hg^{2+}, Ni^{2+}, Pb^{2+}, K^{+} and Zn^{2+} which reveals that none or poor affinities of these metal ions towards the probe. However, addition of Cu^{2+} induced dramatic increase in the fluorescence maxima of PDB at 410 nm. The observed fluorescence enhancement can be attributed to the formation of a complex between Cu^{2+} ions and lone Pair electrons of imine nitrogen of PDB molecule. The fluorescence spectra of PDB with various concentrations of Cu^{2+} were also studied and shown in the Fig. 6b. As can be seen in the figure, the fluorescence emission of PDB decreased by increasing the concentration of Cu^{2+} ions. The fluorescence quenching might be due to the electron transfer between phthalimide derivative and the Cu^{2+} ion [33].

Selective Binding of Cu^{2+}

Competition experiments were also conducted with a purpose to validate the selectivity of PDB for Cu over other tested metal ions. The fluorescence intensity of PDB (10 μM) caused by Cu^{2+}, (5 equiv) and other metal ions (5 equiv.) such as

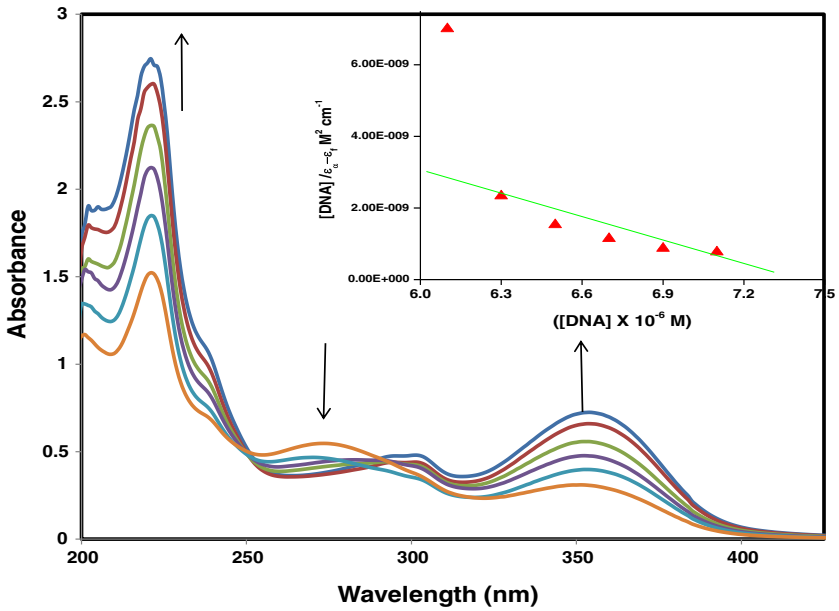

Fig. 9 UV–vis. absorption spectra of compound PDB (4.2×10^{-5} M, *red*) in the presence of increasing amount of Ct-DNA ($6.1–7.1\times10^{-6}$ M). The *arrow* indicates the absorbance change upon increasing DNA concentration. The *inset* is plot of DNA concentration/ $(\varepsilon_a - \varepsilon_f)$ vs DNA concentration for the titration of DNA to compound (PDB)

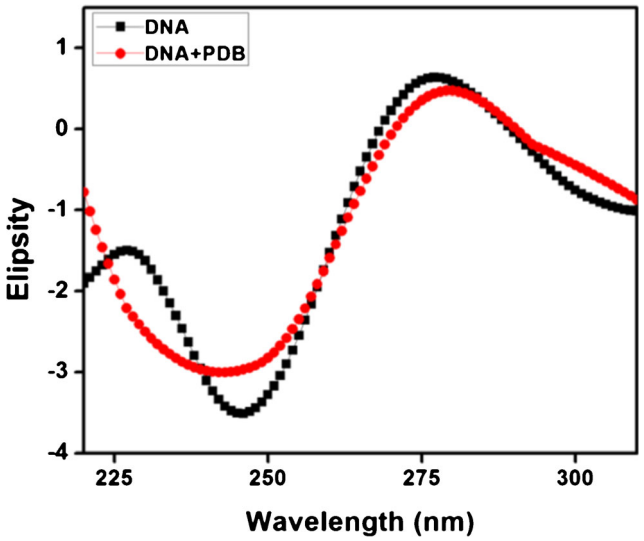

Fig. 10 CD spectra of Ct-DNA (25 mM) in the absence and presence of the compound PDB (25 mM), in 5 mM phosphate buffer

Ba^{2+}, Cd^{2+}, Co^{2+}, Hg^{2+}, Ni^{2+}, Pb^{2+} and Zn^{2+} in DMF/H_2O were demonstrated in Fig. 7b. It can be clearly seen that Cu^{2+} induced fluorescence enhancement was not significantly interfered by other metal ions. These findings clearly indicate that PDB shows high selectivity toward Cu^{2+} over other competitive metal ions.

To further investigate the stoichiometry of the complex, Job's method for absorbance measurement was applied with a total concentration of 1×10^{-5} mol L^{-1} Cu^{2+} and PDB. A plot of $[Cu^{2+}]/\{[Cu^{2+}]+[PDB]\}$ versus the molar fraction of Cu^{2+} was provided in Fig. 8. It was observed that the maximum absorbance was obtained at 0.66, indicating a 1:2 stoichiometry of the Cu^{2+} to PDB in the complex.

DNA Binding Studies

Absorption Measurements

The interaction of compound PDB with Ct-DNA was studied by titrating a constant concentration of PDB with increasing concentration of DNA. The absorption spectra of PDB exhibited two characteristic absorption bands. It was observed that the absorbance intensity of PDB at 350 nm increased gradually without any significant shift of the peak with the increasing concentration of Ct-DNA (Fig. 9). The absorption spectra of the compound PDB exhibited hyperchromism of 36.14 % at 350 nm respectively. In particular, hypochromism and hyperchromism are the spectral features observed during the spectrophotometric titration of small molecules with Ct-DNA [34]. It was reported that hyperchromic effect occurs due to the breakage of the DNA duplex secondary structure whereas hypochromic effect results from contraction of DNA in the helix. The results obtained from the UV titration experiments suggested that the compound bind to Ct-DNA probably via groove binding modes and the binding caused a slight perturbation to the Ct-DNA molecule [35].

In order to get insight into the DNA binding strength of this compound, the intrinsic binding constant K_b was calculated using the following equation [36].

$$\frac{[DNA]}{(\varepsilon_a-\varepsilon_f)}=\frac{[DNA]}{(\varepsilon_b-\varepsilon_f)}+\frac{1}{K_b}(\varepsilon_b-\varepsilon_f)$$

Where, [DNA] is the concentration of DNA in base pairs, ε_a is the extinction coefficient observed for the compound at the given DNA concentration, ε_f is the extinction coefficient of the

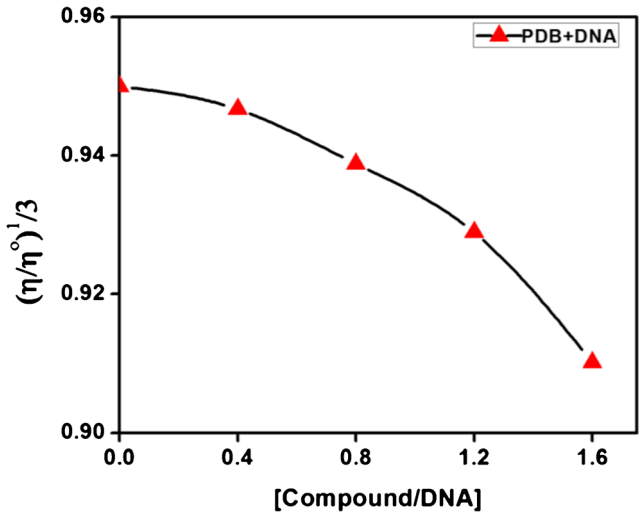

Fig. 11 Effect of increasing amount of PDB on the relative viscosity of DNA at pH 7.4 and 25 °C, [DNA]=4×10^{-5} M and [compound]=0.4 – 1.6×10^{-5} M

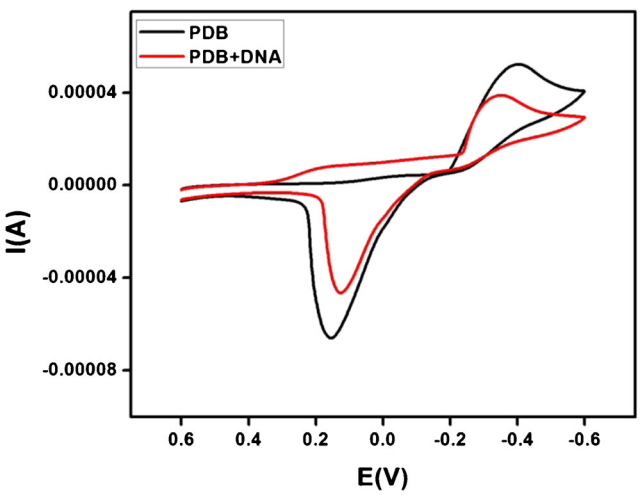

Fig. 12 Cyclic voltammograms of 3.5×10^{-4} M of compound PDB in 50 mM Tris-buffer, pH 7.5 at 50 mV s^{-1} scan rate without DNA (*black*) and with DNA (*red*)

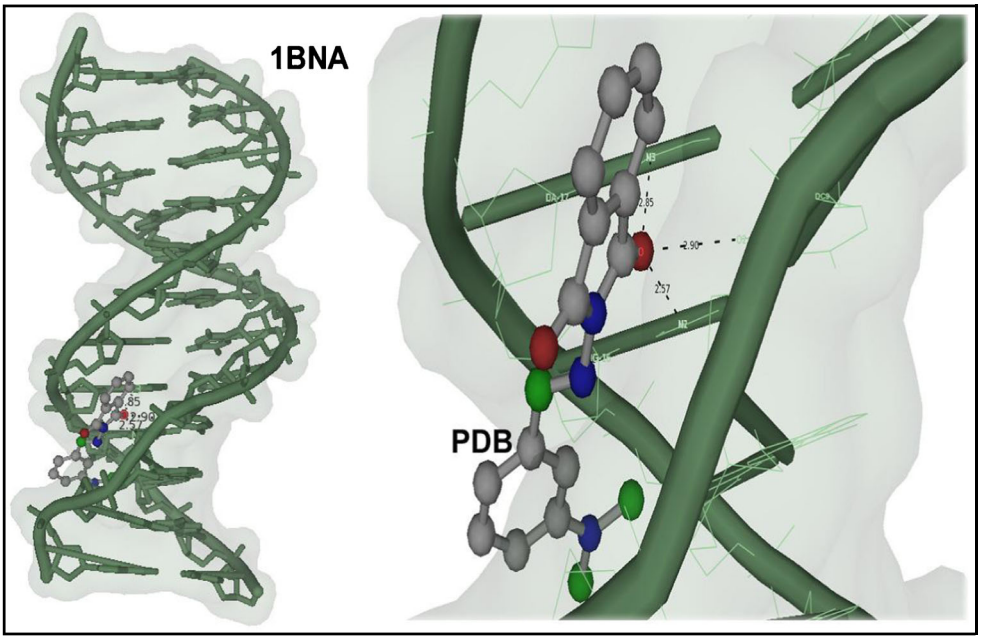

Fig. 13 Molecular docked model of the most favourable binding site of compound (PDB) with DNA dodecamer duplex of sequence $d(CGCGAATTCGCG)_2$ (PDB ID: 1BNA)

compound free in solution, and ε_b is the extinction coefficient of the compound when fully bound to DNA. A plot of [DNA]/($\varepsilon_a - \varepsilon_f$) versus [DNA] gave a slope $1/(\varepsilon_b - \varepsilon_f)$ and Y intercept equal to $1/K_b$ ($\varepsilon_b - \varepsilon_f$) respectively. The intrinsic binding constant K_b is the ratio of the slope to intercept.

The K_b value for compound PDB was calculated and found to be $1.53 \times 10^5\ M^{-1}$, suggesting that PDB has a strong binding affinity for Ct- DNA.

Circular Dichroism Spectra Studies

CD spectroscopy is most useful technique has been used to study the changes in DNA morphology during drug–DNA interactions. The CD spectra of the compound in the absence and presence of Ct-DNA are illustrated in Fig. 10. The characteristic CD spectrum of B-form DNA mainly consists of a positive band at 275 nm (due to base stacking) and a negative band at 245 nm (due to helicity) [37]. In general, electrostatic and groove binding have little or no effect on DNA base stacking and helicity whereas, intercalative binding affects both the positive and negative bands [38]. As depicted in the Fig. 10, a moderate decrease in both the positive and negative bands was observed with no significant change in the band shape. The test compound induced certain conformational changes of the DNA helix, such as the transformation from a B-like to a C-like structure. Considering that the binding of PDB has little effect on the CD spectra of DNA, it can be concluded that the binding mode of PDB to DNA might be electrostatic or groove binding.

Viscosity Measurements

To further investigate the interaction of compound (PDB) with Ct-DNA, viscosity measurements were carried out to observe the hydrodynamic changes of DNA with the addition of increasing concentrations of compound. The effects of the test compound on the viscosity of Ct-DNA are shown in Fig. 11. Intercalative binding of small molecules into DNA base pairs leads to elongation and/or rigidification of the double helix, which resulted in a significant increment in DNA viscosity while partial and/or non-classical intercalation trend to bend or kink of the DNA helix, resulting reduction in its effective length, thereby decrease in viscosity [39]. As illustrated in the Fig. 11, the viscosity of Ct-DNA decreased steadily with increasing concentrations of the compound, indicating that the compound may interact with Ct-DNA by non-intercalative mode. The viscosity result clearly reveals that this compound binds to DNA through groove binding correlated well the results obtained from UV–Vis. and CD spectroscopy.

Electrochemical Studies

The typical cyclic voltammograms of compound (PDB) in the absence and presence of nucleic acids in Tris–HCl buffer

Table 2 Molecular docking parameters of PDB with B-DNA dodecamer duplex (PDB ID: 1BNA)

Compound	ΔG (kcal/mol)	$E_{\text{inter-mol}}$ (kcal/mol)	E_{elec} (kcal/mol)	$E_{\text{torsional}}$ (kcal/mol)	Cluster rmsd	Reference rmsd	NB involved in bonding
PDB	−7.70	−8.17	0.04	0.82	0.00	26.14	DC-9, DG-16, DA-17

solutions are shown in Fig. 11. It has been reported that intercalation causes positive shift in electrochemical potential whereas electrostatic interaction trend to the negative shift in the peak potential [40]. As shown in the Fig. 12, the peak current was dropped by 31 % for compound PDB with significant negative shift in peak potential. The drop in peak current on addition of Ct-DNA can be credited to the slower mass transfer of the compounds bound to DNA, which leads to a decrease in concentration of the free compound in solution [41].

Moreover, negative shifts in peak potential are indicative of groove binding of test compound with the Ct-DNA [42]. Thus, the results obtained from electrochemical studies further support the results of hydrodynamic measurements, UV–Vis and CD spectral studies.

Molecular Docking Studies

Molecular docking analysis of PDB was carried out against dodecamer d(CGCGAATTCGCG)$_2$ (PDB ID: 1BNA). The binding modes of compound were shown in Fig. 13. As illustrated in the figure the carbonyl oxygen of phthalimide of PDB displayed a strong hydrogen-bonding interaction with DNA bases. In addition, test compound exhibited additional stabilization through hydrophobic and van der Waals interactions with nearby nucleotides. The summary of docking results was reported in Table 2. The results of the docking studies reveal that compound (PDB) fit in the minor groove region (C9/G16A17) and the minimum binding energy was calculated to be −7.70 kcal/mol, indicating that the molecule has made stronger interactions with the B-DNA. As a consequence, it can be concluded that compound (PDB) is a promising candidate for further study as potential anticancer agent. The encouraging results from the DNA binding and docking studies impelled us to go for anticancer and antimicrobial studies of the synthesized compound and further studies are in progress.

Conclusions

In summary, we have developed a novel phthalimide-based chemosensor sensitive to solvent polarity, pH and selective to Cu^{2+} ions. The structural characterization of the synthesized compound was determined by elemental analysis, IR, ^{1}H NMR, ^{13}C NMR and electronic spectral analysis. The relative intensity of fluorescence emission maxima depending on solvent polarity, suggesting the compound (PDB) would be able to act as solvent polarity sensor. The fluorescence intensity of PDB is quenched at a lower pH when the azomethine group is protonated, while it increases very sharply from 2 to 6. Further, upon increasing the pH of the solution the quenching of the fluorescence intensity was noticed, demonstrating the high potential of the compound to act as an effective "off–on– off" switch for pH. The interaction of PDB with Ct-DNA was studied in detail by different spectroscopic techniques and the evidences have suggested that the compound could interact with DNA via groove binding. The docking results indicated that the test compound have shown good affinity towards the target receptor.

ACN Acetonitrile, *ACT* Acetone, *Ct-DNA* Calf-thymus DNA, *CD* Circular dichroism, *CYH* Cyclo hexane, *DEE* Diethyl ether, *DMF* Dimethyl formamide, *DMSO* Dimethyl sulfoxide, *DNA* Deoxyribonucleic acid, *ICT* Intra molecular charge transfer

Acknowledgments The financial support from University Grant Commission (Major Research Project, F.No. 41-238/2012) and Department of Science and Technology, New Delhi (Fast Track Scheme for Young Scientist, SR/FT/CS-002/2009) is gratefully acknowledged. Mr. Nayab is grateful to UGC, New Delhi for the financial support through UGC- BSR Fellowship.

References

1. Robinson NJ, Winge DR (2010) Copper metallochaperones. Annu Rev Biochem 79:537–562
2. Liu GL, Feng DQ, Chen T, Li D, Zheng W (2012) DNA-templated formation of silver nanoclusters as a novel light-scattering sensor for label-free copper ionsdetection. J Mater Chem 22:20885–20888
3. Liu Y, Liang P, Guo L (2005) Nanometer titanium dioxide immobilized on silica gel as sorbent for preconcentration of metal ions prior to their determination by inductively coupled plasma atomic emission spectrometry. Talanta 68:25–30
4. Becker JS, Matusch A, Depboylu C, Dobrowolska J, Zoriy MV (2007) Quantitative imaging of selenium, copper, and zinc in thin sections of biological tissues (Slugs-Genus Arion) measured by laser ablation inductively coupled plasma mass spectrometry. Anal Chem 79:6074–6080
5. Gonzales APS, Firmino MA, Nomure CS, Rocha FRP, Oliveira PV, Gaubeur I (2009) Peat as a natural solid-phase for copper preconcentration and determination in a multicommuted flow system coupled to flame atomic absorption spectrometry. Anal Chim Acta 636:198–204
6. Wang J, Xiea Y, Wang Z, Song QH (2014) A highly sensitive and selective naked-eye probe for detecting copper ion based on 2,3-modified Bodipy derivatives. Sens Actuators B 194:149–155
7. Goswami S, Maity S, Das AK, Maity AC (2013) Single chemosensor for highly selective colorimetric and fluorometric dual sensing of Cu(II) as well as 'NIRF' to acetate ion. Tetrahedron Lett 54:6631–6634
8. Perez-Ruiz R, Dıaz Y, Goldfuss B, Hertel D, Meerholz K, Griesbeck AG (2009) Fluoride recognition by a chiral urea receptor linked to a phthalimide chromophore. Org Biomol Chem 7:3499–3504
9. Mohamed RR, Fekry AM (2011) Antimicrobial and anticorrosive activity of adsorbents based on chitosan Schiff's base. Int J Electrochem Sci 6:2488–2508
10. De Clercq B, Verpoort F (2003) Atom transfer radical polymerization of vinyl monomers mediated by a new class of neutral and cationic ruthenium alkylidene catalysts containing a 1,3-dimesityl-4,5-dihydroimidazol-2-ylidene and a Schiff base ligand. Polym Bull 50:153–160

11. Wang PH, Keck JG, Lien EJ, Lai MM (1990) Design, synthesis, testing, and quantitative structure-activity relationship analysis of substituted salicylaldehyde Schiff bases of 1-amino-3-hydroxyguanidine tosylate as new antiviral agents against coronavirus. J Med Chem 33(2):608–614
12. Kumar J, Bhattacharyya PK, Das DK (2015) New duel fluorescent "on–off" and colorimetric sensor for copper (II): Copper (II) binds through N coordination and pi cation interaction to sensor. Spectrochim Acta A 138:99–104
13. Shellaiah M, Wu YH, Singh A, Raju MVR, Lin HC (2013) Novel pyrene- and anthracene-based Schiff base derivatives as Cu^{2+} and Fe^{3+} fluorescence turn-on sensors and for aggregation induced emissions. J Mater Chem A 1:1310–1318
14. Lu F, Gao L, Li H, Ding L, Fang Y (2007) Molecular engineered silica surfaces with an assembled anthracene monolayer as a fluorescent sensor for organic copper(II) salts. Appl Surf Sci 253: 4123–4131
15. Santos JL, Yamasaki PR, Chin CM, Takashi CH, Pavan FR, Leite CQF (2009) Synthesis and in vitro anti Mycobacterium tuberculosis activity of a series of phthalimide derivatives. Bioorg Med Chem 17:3795–3799
16. Lee NJ, Lee SJ, Kim SH, Kang YS, Moon SB, Sohn H, Kang KT, Theodorakis EA (2004) Synthesis and in vitro antitumor activity of phthalimide-based polymers containing camptothecin. Eur Polym J 40:1291–1296
17. Abdel-Aziz AAM (2007) Novel and versatile methodology for synthesis of cyclic imides and evaluation of their cytotoxic, DNA binding, apoptotic inducing activities and molecular modelling study. Eur J Med Chem 42:614–626
18. Sarkar M, Banthia S, Samanta A (2007) A highly selective 'off–on' fluorescence chemosensor for Cr(III). Tetrahedron Lett 47:7575–7578
19. Sarkar M, Yellampalli R, Bhattacharya B, Kanaparthi R, Samanta A (2007) Ratiometric fluorescence signalling of fluoride ions by an amidophthalimide derivative. J Chem Sci 119:91–97
20. Perez-Ruiz R, Griesbeck AG, Sampedro D (2012) Computational study on fluoride recognition by an urea-activated phthalimide chemosensor. Tetrahedron 68:5724–5729
21. Zhong W, Yu JS, Liang Y (2003) Chlorobenzylidine-herring sperm DNA interac-tion: binding mode and thermodynamic studies. Spectrochim. Acta A 59:1281–1288
22. Wang X, Li Y, Gong S, Fu D (2002) A spectroscopic study on the DNA binding behaviour of the anticancer drug dacarbazine. Spectrosc Lett 35:751–756
23. Sandstrom K, Warmlander S, Leijon M, Graslund A (2003) ^{1}H NMR studies of selec-tive interactions of norfloxacin with double-stranded DNA. Biochem Biophys Res Commun 304:55–59
24. Palecek E (2002) Past, present and future of nucleic acids electrochemistry. Talanta 56:809–819
25. Jangir DK, Charak S, Mehrotra R, Kundu S (2011) FTIR and circular dichroism spectroscopic study of interaction of 5-fluorouracil with DNA. J Photoch Photobiol B105:143–148
26. Vaidyanathan VG, Nair BU (2003) Oxidative cleavage of DNA by tridentate copper (II) complex. J Inorg Biochem 93:271–276
27. Huang SY, Zou X (2010) Advances and challenges in protein-ligand docking. Int J Mol Sci 11:3016–3034
28. Morris GM, Goodsell DS, Halliday RS, Huey R, Hart WE, Belew RK, Olson AJ (1998) Automated docking using a Lamarckian genetic algorithm and an empirical binding free energy function. J Comput Chem 19:1639–1662
29. Mouilleron S, Badet-Denisot MA, Golinelli-Pimpaneau B (2008) Ordering of C-terminal loop and glutaminase domains of glucosamine-6-phosphate synthase promotes sugar ring opening and formation of the ammonia channel. J Mol Biol 377(4): 1174–1185
30. Tanak H, Agar AA, Buyukgungor O (2014) Experimental (XRD, FT-IR and UV–Vis) and theoretical modeling studies of Schiff base (E)-N^{1}-((5-nitrothiophen-2-yl) methylene)-2-phenoxyaniline. Spectrochim Acta A 118:672–682
31. Bojinov VB, Georgiev NI, Bosch P (2009) Design, synthesis of highly photostable yellow–green emitting 1,8-naphthalimides as fluorescent sensors for metal cations and protons. J Fluoresc 19: 127–139
32. Liu SB, Bi CF, Fan YH, Zhao Y, Zhang PF, Luo Q, Zhang D (2011) Synthesis, characterization and crystal structure of a new fluorescent probe based on Schiff base for the detection of Zinc(II). Inorg Chem Commun 14:1297–1301
33. Aksuner N, Henden E, Yilmaz I, Cukurovali A (2009) A highly sensitive and selective fluorescent sensor for the determination of copper(II) based on a schiff base. Dyes Pigments 83:211–217
34. Icsel C, Yilmaz VT (2014) In vitro DNA binding studies of the sweetening agent saccharin and its copper(II) and zinc(II) complexes. J Photoch Photobiol B 130:115–121
35. Zeglis BM, Pierre VC, Barton JK (2007) Metallo-intercalators and metallo-insertors. Chem Commun 28:4565–4579
36. Hu H, ChenY ZH, Pan Z (2011) Synthesis, crystal structure, and DNA cleavage activity of a dinuclear nickel(II) complex with a macrocyclic ligand. Trans Met Chem 36:395–402
37. Ivanov VI, Minchenkova LE, Schyolkina AK, Poletayer AI (1973) Different conformations of double-stranded nucleic acid in solution as revealed by circular dichroism. Biopolymers 12:89–110
38. Chen LM, Liu J, Chen JC, Shi S, Tan CP, Zheng KC, Ji LN (2008) Experimental and theoretical studies on the DNA-binding and spectral properties of water-soluble complex $[Ru(MeIm)4(dpq)]^{2+}$. J Mol Struct 881:156–166
39. Wu H, Yuan J, Bai Y, Pan G, Wang H, Kong J, Fan X, Liu H (2012) Synthesis, structure, DNA-binding properties and antioxidant activity of silver(I) complexes containing V-shaped bis-benzimidazole ligands. Dalton Trans 41:8829–8838
40. Zhang SS, Niu SY, Qu B, Jie GF, Xu H, Ding CF (2005) Studies on the interaction mechanism between hexakis(imidazole) manganese(II) terephthalate and DNA and preparation of DNA electrochemical sensor. J Inorg Biochem 99:2340–2347
41. Hirohama T, Kuranuki Y, Ebina E, Sugizaki T, Arii H, Chikira M, Selvi PDB, Palaniandavar M (2005) Copper(II) complexes of 1,10-phenanthroline-derived ligands: studies on DNA binding properties and nuclease activity. J Inorg Biochem 99:1205–1219
42. Carter MT, Rodriguez M, Bard AJ (1989) Voltammetric studies of the interaction of metal chelates with DNA. 2. tris-chelated complexes of cobalt (III) and iron (II) with 1,10-phenanthroline and 2, 2′-bipyridine. J Am Chem Soc 11:8901–8911